doi:10.1016/j.jmb.2010.12.029 J. Mol. Biol. (2011) xx, xxx–xxx

Contents lists available at www.sciencedirect.com

Journal of Molecular Biology

journal homepage: http://ees.elsevier.com.jmb

The Effect of Parkinson's-Disease-Associated Mutations on the Deubiquitinating Enzyme UCH-L1

Fredrik I. Andersson[1], Elizabeth F. Werrell[1], Lindsay McMorran[1], William J. K. Crone[1], Chittarnajan Das[2], Shang-Te Danny Hsu[1,3]* and Sophie E. Jackson[1]*

[1]*Department of Chemistry, University of Cambridge, Lensfield Road, Cambridge CB2 1EW, UK*
[2]*Department of Chemistry, Purdue University, 560 Oval Drive, West Lafayette, IN 47907, USA*
[3]*Institute of Bioinformatics and Structural Biology, National Tsing Hua University, 101, Section 2, Kuang-Fu Road, Hsinchu 30013, Taiwan*

Received 21 August 2010; received in revised form 15 December 2010; accepted 20 December 2010

Edited by C. R. Matthews

Keywords:
ubiquitination;
deubiquitination;
protein stability;
mutation;
Parkinson's disease

The neuronal ubiquitin C-terminal hydrolase (UCH) UCH-L1 has been linked to Parkinson's disease (PD) and other neurodegenerative diseases. Here, we present a study on the structure, stability, unfolding, and dynamics of wild-type and mutant UCH-L1. Fluorescence, far-UV CD, and NMR measurements were used to establish that the unfolding of UCH-L1 is three-state under equilibrium conditions and that an intermediate is populated. S18Y and I93M mutants, which are associated with a decreased risk or an increased risk of PD, respectively, are less stable than wild type. However, while there is minimal structural perturbation in the S18Y mutant, the I93M mutation is more disruptive. In particular, the NMR data suggest that there are local rearrangements around the site of the mutation, which we propose results in the exposure of hydrophobic surface area. This may have two consequences: an increased tendency towards, firstly, aggregation *in vivo*, and, secondly, aberrant interactions with tubulin and the chaperone-mediated autophagy machinery as observed by other groups, both of which may be involved in neurodegenerative processes.

Introduction

Deubiquitinating enzymes hydrolyze the ε-linked/α-linked amide bonds formed between ubiquitin and target proteins or small-molecule nucleophiles and have many functions.[1–3] They play important roles in many cellular processes, including proteasomal and lysosomal protein degradation, trafficking, DNA damage response and DNA repair, endoplasmic-reticulum-associated protein degradation, cell cycle regulation, and kinase modification.[4] The human genome encodes approximately 95 deubiquitinating enzymes[5] in five major classes, including ubiquitin C-terminal hydrolases (UCHs).

UCH-L1 is a member of the UCH family and is highly expressed normally in neurons and testes; however, it has also been shown to be expressed abnormally in lung cancer lines and colorectal cancer.[6–8] UCH-L1 is expressed at high levels in neurons, constituting up to 2% of the total soluble proteins,[9] and although the role of UCH-L1 in normal cells is not well understood, it has been shown to play a role in normal synaptic function: pharmacological inhibition of UCH-L1 has been

**Corresponding authors.* S.-T. D. Hsu is to be contacted at Institute of Bioinformatics and Structural Biology, National Tsing Hua University, 101, Section 2, Kuang-Fu Road, Hsinchu 30013, Taiwan. E-mail addresses: sthsu@life.nthu.edu.tw; sej13@cam.ac.uk.

Abbreviations used: UCH, ubiquitin C-terminal hydrolase; PD, Parkinson's disease; gad, gracile axonal dystrophy; Aβ, amyloid β-protein; AD, Alzheimer's disease; MD, molecular dynamics; HDX, hydrogen/deuterium exchange; SEC, size-exclusion chromatography.

0022-2836/$ - see front matter

shown to significantly reduce monomeric ubiquitin levels and to cause alterations in synaptic protein distribution and spine morphology.[10] In addition, loss of function of UCH-L1 in mice (by an in-frame deletion of exons 7 and 8) caused a gracile axonal dystrophy (gad) phenotype in which there was sensory–motor ataxia.[11] The gad mice also showed axonal degeneration and formation of spheroid bodies in nerve terminals and an accumulation of amyloid β-protein (Aβ) and ubiquitin-positive deposits, suggesting that UCH-L1 is involved in neurodegenerative disorders.[11] Recently, UCH-L1 has been shown to restore dendritic spine density in hAPP transgenic mice, which show acute alterations to dendritic spines induced by Aβ.[12]

In addition to their possible role with Aβ, two mutations that have been associated with a decreased susceptibility to Parkinson's disease (PD) (S18Y) or with an autosomal dominant form of PD [I93M (PARK5)] have been identified in UCH-L1.[13] The association of the S18Y polymorphism with PD is somewhat controversial, and results from different studies have produced conflicting results (see Supporting Information). However, the I93M mutant has been identified from a study of a German family with PD, and it has been shown to have a slightly lower catalytic activity towards model-ubiquitinated substrates compared to wild type.[13] Overexpression of α-synuclein significantly enhanced the loss of nigral dopaminergic cells in UCH-L1 I93M transgenic mice, but had little effect on age-matched UCH-L1 wild-type mice, nontransgenic littermates, or gad mice that lack UCH-L1, suggesting that I93M may cause a gain of toxic function.[14] Patients with sporadic PD show both α-synuclein and UCH-L1 double-positive Lewy bodies in nigral dopaminergic neurons, suggesting a possible physical interaction between the two proteins.[15]

In addition to mutations, chemical modification of UCH-L1—including carbonyl modification by the reaction of UCH-L1 with reactive aldehyde species—has also been shown to be elevated in the brains of patients with both PD and Alzheimer's disease (AD).[16] Recently, the reactivity of mouse UCH-L1 towards the α,β-unsaturated carbonyl, cyclopentenone prostaglandin 15d-PGJ2, has been investigated.[17] In this case, 15d-PGJ2 was shown to specifically modify Cys152 in wild-type and I93M UCH-L1, and the resulting modified protein was shown to aggregate under the conditions used.[17]

The structure of UCH-L1 contains a central β-sheet that is flanked on either side by α-helices (Fig. 1a). In the crystal structure, UCH-L1 is an asymmetric dimer; however, equilibrium sedimentation analysis showed that the protein is monomeric in solution.[18] The catalytic triad comprises Cys90, His161, and Asp176; in the crystal structure, the side chains of these residues are not close enough for catalytic activity, suggesting that in the absence of substrate, UCH-L1 is in an inactive form. In addition, the active site is covered by a loop (L8) that has been suggested to restrict the size of substrates that can access the active-site cleft.[18] The protein has an unusual knotted topology that is created by five crossings of the polypeptide chain, giving rise to a 5_2 or Gordian knot (Fig. 1b).[19]

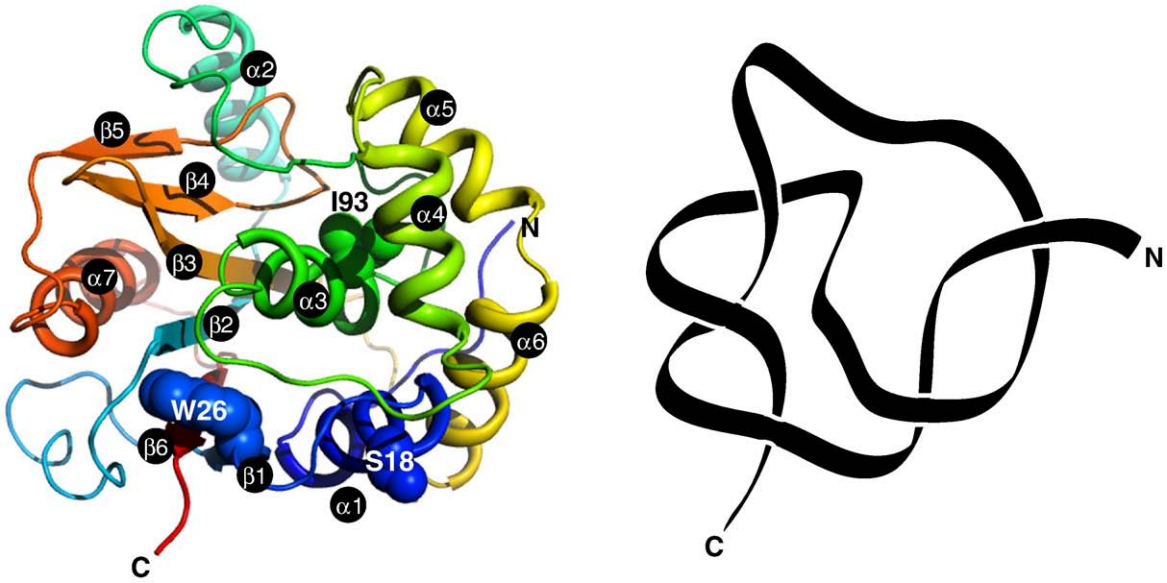

Fig. 1. Structure of human UCH-L1. (a) Ribbon diagram showing the backbone structure of UCH-L1, with the side chains of residues Ser18 (blue), Trp26 (blue), and Ile93 (green) shown in space-filling mode. (b) Simplified representation of the polypeptide chain showing the five topological crossings that give rise to the 5_2 Gordian knot topology.

Please cite this article as: Andersson, F. I. *et al.*, The Effect of Parkinson's-Disease-Associated Mutations on the Deubiquitinating Enzyme UCH-L1, *J. Mol. Biol.* (2011), doi:10.1016/j.jmb.2010.12.029

Following on from our previous work on the folding and stability of human UCH-L3[20] and the recently published backbone NMR assignment of human UCH-L1,[21] we have undertaken a detailed biophysical analysis of the wild-type, S18Y, and I93M forms of UCH-L1 in order to assess the effects of the two mutations on the stability, unfolding, structure, and dynamics of the protein. Fluorescence, far-UV circular dichroism (CD), and NMR were used as the main probes of structure and dynamics, and the stability and unfolding of the proteins were measured using chemical denaturants.

Results

Reversible chemical denaturation of wild-type and mutant UCH-L1

The stabilities of wild-type and mutant UCH-L1 were assessed using chemical denaturation, and the unfolding of the protein was probed using intrinsic fluorescence and far-UV CD. Denaturation was found to be fully reversible under the conditions used. In wild-type UCH-L1, there is a single tryptophan (Trp26) and two tyrosines (Tyr80 and Tyr173); therefore, the tryptophan dominates the emission spectrum, so the fluorescence data largely report on the local environment of Trp26. A careful inspection of fluorescence emission scans taken at different denaturant concentrations reveals a complex behavior—at around 3 M urea, a shift in λ_{max} from 310 to 340 nm is observed; however, at higher concentrations of denaturant, we see a second transition in which λ_{max} redshifts further to 355 nm, indicative of the population of an intermediate state (Fig. S1). The data shown in Fig. 2a–c for wild-type and mutant UCH-L1 were globally fitted to a three-state model, and the thermodynamic parameters obtained are shown in Table 1. In contrast, the unfolding data monitored using far-UV CD showed only a single sharp transition, which

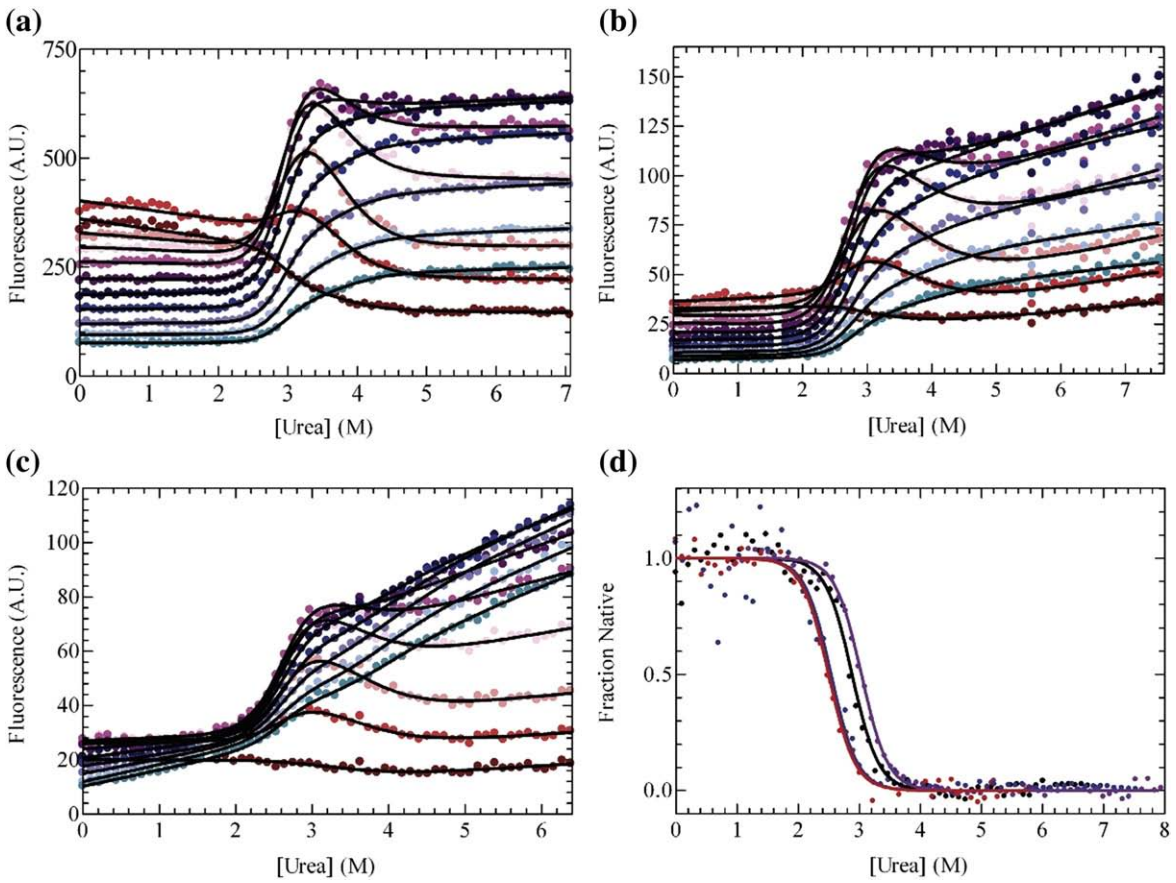

Fig. 2. Measurements of the thermodynamic stabilities of wild-type and mutant UCH-L1. Urea denaturation curves using intrinsic fluorescence to probe unfolding. The data show different wavelength measurements: 300 nm (dark red), 310 nm (red), 320 nm (pink), 330 nm (light pink), 340 nm (magenta), 350 nm (purple), 360 nm (navy blue), 370 nm (blue), 380 nm (grey blue), 390 nm (sky blue), 400 nm (teal). The continuous line shows the best fit of the data to a three-state model. (a) Wild type. (b) S18Y. (c) I93M. (d) Urea denaturation curves for wild-type (black and purple circles), I93M (blue circles), and S18Y (red circles) using far-UV CD to probe unfolding. The continuous line shows the best fit of the data to a two-state model.

Please cite this article as: Andersson, F. I. *et al.*, The Effect of Parkinson's-Disease-Associated Mutations on the Deubiquitinating Enzyme UCH-L1, *J. Mol. Biol.* (2011), doi:10.1016/j.jmb.2010.12.029

Table 1. Thermodynamic parameters for the reversible unfolding of wild-type and mutant UCH-L1 under equilibrium conditions

	Wild type			
Thermodynamic parameters	Unfolding	Refolding	S18Y	I93M
Fluorescence				
m_{I-N} (kcal mol^{-1} M^{-1})	3.05 ± 0.02	3.23 ± 0.05	2.35 ± 1.05	3.03 ± 0.05
$[D]^{50\%}_{I-N}$ (M)	2.95 ± 0.002	3.02 ± 0.004	2.78 ± 0.008	2.67 ± 0.004
$\Delta G^{H_2O}_{I-N}$ (kcal mol^{-1})[a]	8.60 ± 0.43	8.80 ± 0.44	8.10 ± 0.41	7.78 ± 0.39
m_{D-I} (kcal mol^{-1} M^{-1})	1.65 ± 0.03	1.71 ± 0.05	1.05 ± 0.05	1.18 ± 0.05
$[D]^{50\%}_{D-I}$ (M)	3.68 ± 0.01	3.62 ± 0.02	3.59 ± 0.04	3.54 ± 0.02
$\Delta G^{H_2O}_{D-I}$ (kcal mol^{-1})[b]	5.14 ± 0.46	5.05 ± 0.45	5.01 ± 0.45	4.94 ± 0.44
Far-UV CD				
m_{D-N} (kcal mol^{-1} M^{-1})	2.96 ± 0.25	3.07 ± 0.36	2.48 ± 0.44	2.75 ± 0.29
$[D]^{50\%}_{D-N}$ (M)	2.91 ± 0.35	2.88 ± 0.48	2.52 ± 0.65	2.50 ± 0.37
$\Delta G^{H_2O}_{D-I}$ (kcal mol^{-1})[c]	7.97 ± 0.99	7.89 ± 1.34	6.90 ± 1.80	6.85 ± 1.04
Fluorescence and far-UV CD (global fit)[d]				
m_{I-N} (kcal mol^{-1} M^{-1})	2.95 ± 0.03			2.93 ± 0.05
$[D]^{50\%}_{I-N}$ (M)	3.00 ± 0.003			2.55 ± 0.005
$\Delta G^{H_2O}_{I-N}$ (kcal mol^{-1})[a]	8.83 ± 0.10			7.47 ± 0.13
m_{D-I} (kcal mol^{-1} M^{-1})	1.83 ± 0.05			1.24 ± 0.06
$[D]^{50\%}_{D-I}$ (M)	3.71 ± 0.01			3.40 ± 0.02
$\Delta G^{H_2O}_{I-N}$ (kcal mol^{-1})[b]	6.80 ± 0.18			4.23 ± 0.20

Fluorescence and far-UV CD data were analyzed using a three-state model and a two-state model, respectively.
[a] Calculated using an average m_{I-N} value of 2.91 ± 0.15 kcal mol^{-1} M^{-1}.
[b] Calculated using an average m_{D-I} value of 1.40 ± 0.13 kcal mol^{-1} M^{-1}.
[c] Calculated using an average m_{D-N} value of 2.74 ± 0.11 kcal mol^{-1} M^{-1}.
[d] Fluorescence and far-UV CD data were globally fitted to a three-state model. The signal between 220 and 240 nm was taken for the far-UV CD data at each denaturant concentration, and between 300–400 nm for fluorescence emission scans. The S18Y data would not fit globally to a three-state model, as the signal-to-noise ratio in the far-UV CD data was not as good as that for wild type or I93M.

fits well to a two-state model (Fig. 2d) [the far-UV CD signal as a function of denaturant concentration did show a change between 4 and 6 M urea after the major unfolding transition, indicative of an additional unfolding event with a smaller signal (Fig. S2); however, the change in signal was not large enough to fit the data to a three-state model]. The thermodynamic parameters obtained from the two-state fit of the far-UV CD data are shown in Table 1 and are in good agreement with the thermodynamic stabilities measured for the first transition (native state to intermediate state) observed in fluorescence experiments. The fluorescence and far-UV CD data sets were also globally fitted together to a three-state model, and the parameters obtained from these fits are also shown in Table 1. The values are all within error of those from the fit of fluorescence and far-UV CD data sets on their own.

Unfolding kinetics of wild-type and mutant UCH-L1

The stabilities of wild-type and mutant UCH-L1 were also probed by measuring the unfolding kinetics. Intrinsic fluorescence was used, and two unfolding phases were observed over a wide range of denaturant concentrations (Fig. 3). In both cases, there is a linear relationship between the natural logarithm of the rate constants and the denaturant concentration, as expected and observed for many proteins.[22] The fact that two unfolding phases are observed is more unusual than the unfolding kinetics that have been published on smaller monomeric proteins; however, multiphase unfolding kinetics have been observed for a number of proteins with more complex unfolding/folding pathways.[23–25] As expected and in agreement with the equilibrium studies, both I93M and S18Y unfold faster than the wild type. Both kinetic phases are affected, and the mutation I93M has a more significant effect than S18Y (Fig. 3).

Structures of wild-type and mutant UCH-L1

Far-UV CD spectra

An initial assessment of the effect of the mutations on the structure of the protein was made based on the far-UV CD spectra of wild-type and mutant UCH-L1 recorded under native conditions (Fig. S3). For S18Y, there is little difference in the spectrum compared to wild type, suggesting that there is minimal perturbation of the structure on mutation. In contrast, for I93M, the far-UV CD of this mutant shows a small but nonetheless significant decrease in secondary structure. To ensure that the effect was real and not an artifact of protein concentration, we determined all protein concentrations using both

Please cite this article as: Andersson, F. I. *et al.*, The Effect of Parkinson's-Disease-Associated Mutations on the Deubiquitinating Enzyme UCH-L1, *J. Mol. Biol.* (2011), doi:10.1016/j.jmb.2010.12.029

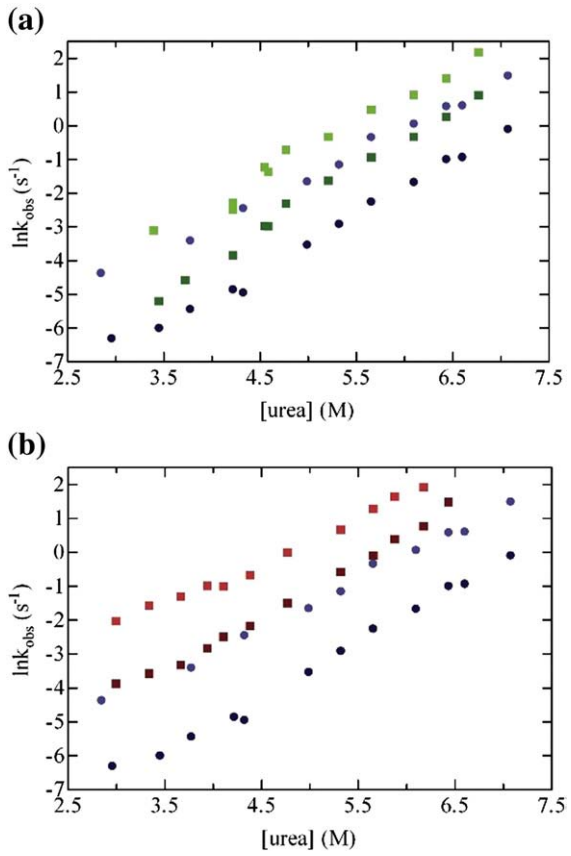

Fig. 3. Unfolding rate constants calculated from the best fit of the unfolding traces for (A) wild type (blue) and S18Y (green) or (B) wild type (blue) and I93M (red) to a double exponential process. The rate constants for both the fast unfolding phase (light blue, light red and light green) and the slow unfolding phase (dark blue, dark red and dark green) are shown as a function of final denaturant concentration.

spectrophotometry and amino acid analysis, performed in triplicate or in duplicate, respectively. The standard deviations were less than 4% for the wild type and the mutant, and the results were also confirmed using different preparations of the protein. An analysis of the secondary structure content of the wild type and the mutant based on the CD results, using the program DichroWeb†, shows that the change in signal observed for I93M can be attributed to a loss of α-helical structure (Fig. S3) that is also observed by other groups.[26] In order to understand the structural changes that occur in the I93M mutant at the residue level, we undertook a series of NMR experiments.

† http://www.cryst.bbk.ac.uk/cdweb/

Solution-state NMR spectroscopy of wild-type and mutant UCH-L1

Changes in NMR chemical shift on mutation

The ^{1}H, ^{13}C, and ^{15}N backbone resonances of wild-type UCH-L1 have been assigned,[21] and these were used as a basis for the assignments of the $^{15}N–^{1}H$ heteronuclear single quantum coherence spectra of S18Y and I93M (Fig. 4a). From these spectra, it can be clearly seen that the majority of chemical shifts of the wild type and the mutants are, in most cases, superimposable, and that relatively few peaks have shifted significantly, indicating that the overall fold of the mutants is the same as that of the wild type. For S18Y, there are very few changes in the chemical shifts ($\langle\Delta\delta\rangle = 0.04 \pm 0.09$ ppm), and these are localized in α-helix 1, α-helix 2, and β-strand 1, which are in proximity to the mutated side chain. In contrast, there are a larger number of chemical shift differences between I93M and wild type ($\langle\Delta\delta\rangle = 0.12 \pm 0.37$ ppm) (Fig. 4b). In this case, the differences observed are not only near the mutated residue but also at sites more distant in sequence—in particular Met82 and Lys83; additionally, Lys131 and Phe133 also exhibit relatively high chemical shift perturbations ($\Delta\delta = 0.71$ and 0.77 ppm, respectively). Structural mapping of the chemical shift perturbations shows that the perturbations are propagated from the mutation site to the preceding loop, the N-terminus, α-helices 5 and 6 that form one of the two crossings of the knotted structure, and one edge of the central β-sheet that faces towards α-helices 5 and 6 (Fig. 4).

In order to investigate the apparent loss of secondary structure on the mutation of Ile93 to Met, as indicated by far-UV CD, we recorded the HNCO and HNCA spectra for I93M to obtain the corresponding C^{α} and CO chemical shifts, respectively, which are generally more sensitive to changes in backbone conformation than are the chemical shifts of $^{15}N–^{1}H$ correlations. While the $^{15}N–^{1}H$ correlations show significant chemical shift perturbations in α-helices 3, 5, and 6 (Fig. 4), the corresponding C^{α} and CO nuclei exhibit relatively limited chemical shift perturbations, except that of Phe133 (located in the center of α-helix 5), which exhibits an upfield shift of 1.24 ppm compared to that of wild type (Fig. S4). Furthermore, the $i–i+n$ backbone amide-to-amide nuclear Overhauser enhancement cross-peaks, which reflect the presence of α-helical conformations, are observed in α-helices 3, 5, and 6 for both wild type and I93M. Thus, while the NMR data do not show the loss of α-helical structure in I93M predicted from the far-UV CD data, ^{1}H, ^{15}N, and ^{13}C experiments clearly indicate that there is some structural perturbation in several of the α-helices on mutation.

In silico modeling, using molecular dynamics (MD) simulations, and an explicit solvent model, using the

Please cite this article as: Andersson, F. I. *et al.*, The Effect of Parkinson's-Disease-Associated Mutations on the Deubiquitinating Enzyme UCH-L1, *J. Mol. Biol.* (2011), doi:10.1016/j.jmb.2010.12.029

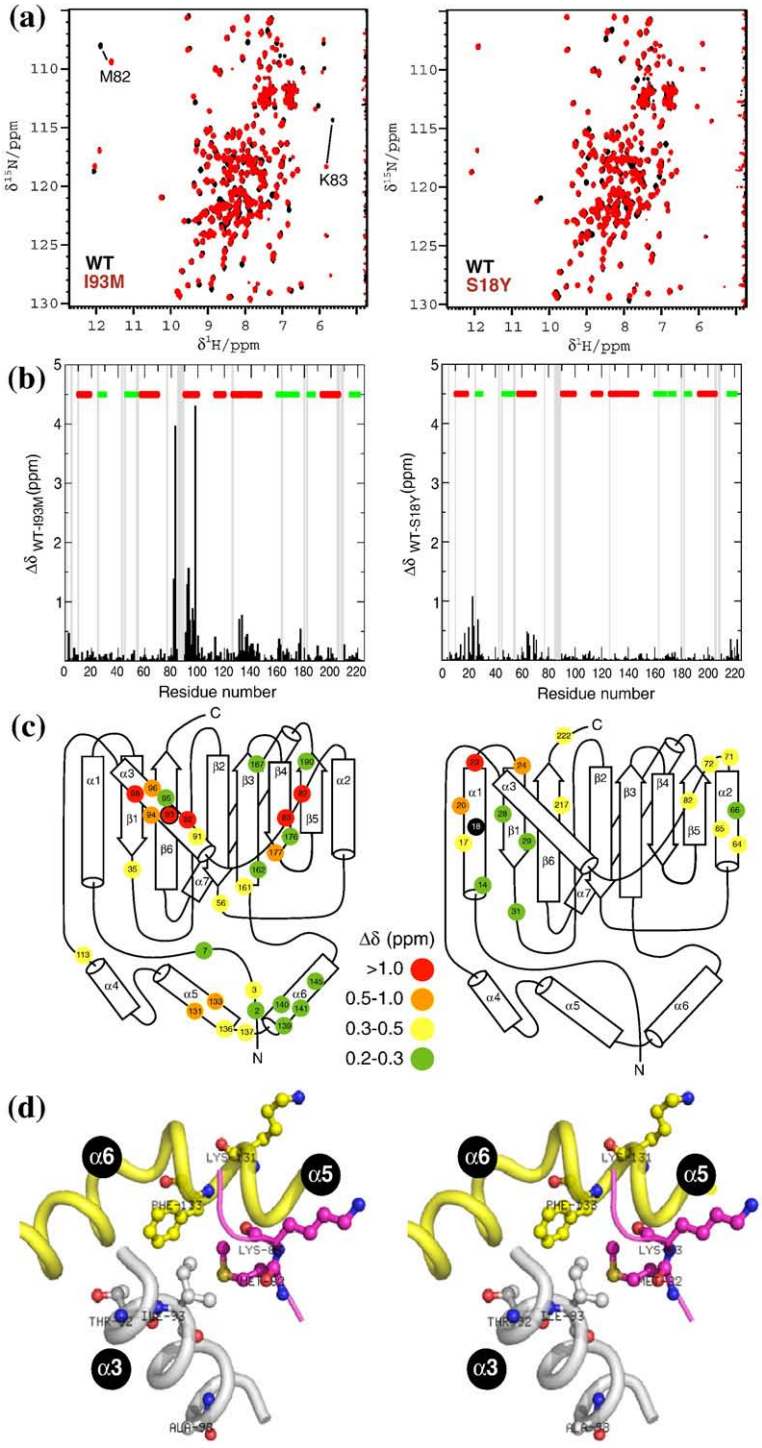

Fig. 4. Structural mapping of chemical shift perturbations in UCH-L1 resulting from the point mutations I93M and S18Y. (a) Overlays of the 500 -MHz ^{15}N–^{1}H heteronuclear single quantum coherence spectra of UCH-L1 (black) and its variants (red), I93M (top) and S18Y (bottom), recorded at 25 °C. The cross-peaks of M82 and K83 that undergo significant chemical shift changes as a result of the I93M mutation are indicated and labeled. (b) Chemical shift perturbations (Δδ) of UCH-L1 variants as a function of residue number. The weighted Δδ is defined as $\sqrt{(\Delta\delta(^{1}H))^2 + (0.65\Delta\delta(^{15}N))^2}$. The sets of residues that form the α-helices and β-strands in the crystal structure are indicated by red and green boxes at the top of the diagram. Gray bars indicate the positions of the residues whose backbone amide ^{15}N–^{1}H correlations were unavailable, including nine prolines. (c) Topological mapping of the chemical shift perturbations of UCH-L1 variants. The positions of the residues that exhibit significant chemical shifts changes are indicated with residue numbers and are color coded accordingly, as shown below. (d) Stereo view of a cartoon representation of the region in UCH-L1 that exhibits significant chemical shift changes upon I93M mutation, as shown in (c). Residues 80–83 are shown in pink, residues 91–102 that form α3 are shown in gray, and residues 129–139 that form α5 and α6 are shown in yellow. The residues that exhibit significant chemical shift perturbations around the I93M mutation site are shown in ball-and-stick representation, and the corresponding identities are indicated.

wild-type crystal structure as the starting point, were performed to try to rationalize these experimental observations and to gain further insight into structural rearrangements in I93M. Both wild type and I93M are stable over the 10-ns simulation trajectories, with subtle conformational fluctuations and changes in their secondary structure contents. We do, however, observe small changes in the intramolecular interaction network, which may account for the observed C^{α} chemical shift change of Phe133 in α-helix 5. In wild-type UCH-L1, the side chain of Ile93 is in contact with the hydrophobic side chain of Met82 while forming backbone-to-backbone hydrogen bonds with Ser89 and His97, which help maintain the structure (Fig. 4d). In I93M, the side chain of Met93 tends to interact with those of Phe133

Please cite this article as: Andersson, F. I. *et al.*, The Effect of Parkinson's-Disease-Associated Mutations on the Deubiquitinating Enzyme UCH-L1, *J. Mol. Biol.* (2011), doi:10.1016/j.jmb.2010.12.029

and Gln84 while maintaining the backbone hydrogen-bond network with Ser89 and His97 (Fig. S5). These subtle and local structural rearrangements between the side chains of Met93, Met82, Lys83, and Phe133 in the I93M variant may therefore account for the observed chemical shift perturbations, but they do not appear to be sufficient to account for the observed changes in the far-UV CD signal for I93M. It is likely that conformational rearrangements on mutation are more global and are on longer timescales than we are able to detect in a relatively short MD simulation. NMR hydrogen/deuterium exchange (HDX) experiments were therefore performed in order to probe the changes in structure and dynamics on longer timescales.

HDX experiments

The HDX rates of amide groups in wild type and I93M were measured, and a wide range of rate constants were obtained. Because the stability of UCH-L1 variants is pH sensitive between pH 6.5 and 8.5, it difficult to establish that the HDX process is under the EX2 regime, which is the condition under which the exchange rates can be converted into the free energy of unfolding of individual residues. Instead, we chose to analyze the HDX data in terms of protection factors, namely the logarithm of the ratio between the intrinsic HDX rates k_{int} and the observed HDX rates k_{ex} [$\log(k_{int}/k_{ex})$]. The slower HDX rates indicate a higher degree of protection of the amide proton, which prevents it from exchanging with bulk solvent. The protection factors calculated for the residues in wild type and I93M are shown in Fig. 5a and b, with the latter illustrating the overall topological structure of the protein. For wild-type UCH-L1, many of the protection factors are greater than 7, and these residues, which are highly protected from solvent exchange, are primarily located in the central β-sheet region of the protein (β-strands 2–4 and 6). However, several residues in α-helices 1, 3, and 7, as well as Leu3 at the N-terminus, are also highly protected (Fig. 5). Note that α-helices 3 and 7 are packed directly against the central β-sheet region. The HDX data suggest that α-helices 1, 3, and 7 may have some residual structure in the intermediate state. However, the data show that these helices are not fully formed and, therefore, these data are compatible with the far-UV CD urea denaturation data, suggesting that much of the helical structure is lost in the intermediate state.

The protection factors for I93M are, in general, much lower than those for wild type (Fig. 5), consistent with the fact that this mutant is some 1 kcal mol^{-1} less stable. The most highly protected

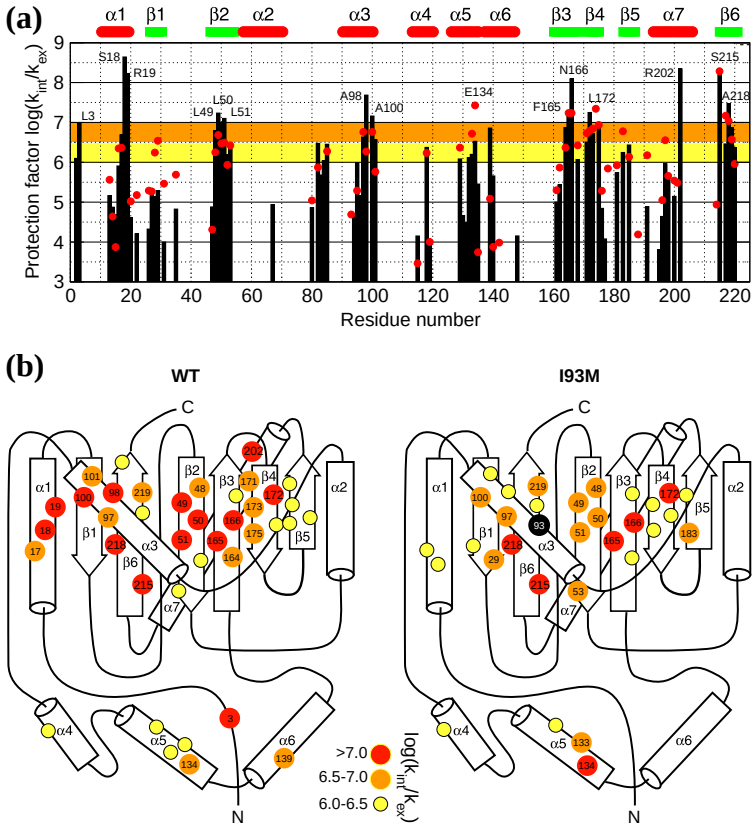

Fig. 5. NMR HDX experiments of UCH-L1. (a) The protection factors for UCH-L1 variants, wild type, and I93M, derived from NMR HDX experiments under native conditions, are shown as a function of residue numbers. The values of wild type and I93M are shown in black bars and filled red circles, respectively. Residues that exhibit high protection factors are labeled with their identities. The sets of residues that form the α-helices and β-strands in the crystal structure are indicated by red and green boxes at the top of the diagram, with labels that are consistent with the nomenclature used in the crystallographic study. (b) Topological mapping of the protected amide groups in wild type (left) and I93M (right). The positions of the residues that exhibit relatively higher protection factors are indicated with residue numbers and are color coded accordingly, as shown below.

Please cite this article as: Andersson, F. I. *et al.*, The Effect of Parkinson's-Disease-Associated Mutations on the Deubiquitinating Enzyme UCH-L1, *J. Mol. Biol.* (2011), doi:10.1016/j.jmb.2010.12.029

amide protons are in the central β-strands 2, 3, 4, and 6. While a residue-by-residue comparison of the results for wild type and I93M shows that the exchange rates that have been most perturbed by mutation are from residues around the mutation site (in α-helix 3 and in the central β-sheet that wraps around α-helix 3), residues 17–19 in α-helix 1 and Leu3 at the N-terminus also exhibit significant increases in exchange rate in I93M. Note that while most residues exhibit lower protection factors in I93M than in wild type, indicating destabilization, there are a number of residues that have higher protection factors, reflecting a local stabilization of structure on mutation (Fig. 5). In particular, Phe133 and Glu134 in I93M show significantly higher protection factors, which we attribute to the aforementioned localized conformational rearrangements involving hydrophobic contacts between the side chains of Phe133 and the Met introduced at position 93.

Hydrodynamics of UCH-L1 and its variants by ^{15}N relaxation dynamics

There have been several reports on a dimeric form of UCH-L1 that has been linked to a novel ubiquitin ligase activity.[27] Here, NMR experiments have been carried out to obtain the ^{15}N longitudinal and transverse relaxation rates (R_1 and R_2) of the wild-type, I93M, and S18Y variants of UCH-L1 in order to monitor the internal dynamics and to derive the corresponding autocorrelation times associated with the oligomeric states of globular proteins. Under the conditions used (i.e., at a protein concentration of 200 μM, at a temperature of 25 °C, and at a proton Lamour frequency of 500 MHz), the apparent correlation times of wild type, I93M, and S18Y, derived from the R_2/R_1 ratios, are 10.9 ± 3.4 ns (n = 177), 12.3 ± 2.7 ns (n = 162), and 9.9 ± 3.1 ns (n = 159), respectively (Fig. S6). On one hand, the correlation time of I93M is statistically longer than that of wild type (p < 0.001), but it is still compatible with a monomeric globular protein of 26 kDa. On the other hand, the relatively long correlation time of I93M suggests that it is slightly more expanded than wild type, which may reflect structural rearrangements or partial unfolding. Likewise, the relatively short correlation time of S18Y would suggest it to be slightly more compact than wild type. To further verify the oligomeric states of UCH-L1 variants, we undertook size-exclusion chromatography (SEC).

Size-exclusion chromatography

The oligomeric state of wild-type and mutant UCH-L1 was assessed using SEC (Fig. S7). Initially, the protein samples were dialyzed overnight at 4 °C into a phosphate buffer, which removes the reducing agent, and then incubated at 37 °C for various times before SEC was performed. For the first time point measured (0 h after dialysis), all the proteins are monomeric, and there is no evidence for dimer or higher oligomers. In the presence of DTT, the monomers are stable. Even in the absence of reducing agents, wild-type UCH-L1 behaves as a monomer in solution and elutes from the size-exclusion column in a volume that corresponds to a molecular mass of 24.8 kDa. For S18Y, there is a very large peak due to a monomer corresponding to a molecular mass of 24.7 kDa, which is very similar to wild type; however, in contrast to wild type, small amounts of dimer and higher oligomers can form over time (Fig. S7). Similar results are found for I93M: the majority of the sample is monomeric and elutes with a molecular mass of 25.3 kDa (slightly higher than wild type), which may reflect the fact that the structure of this mutant is more expanded due to small structural rearrangements around the site of mutation. These results suggest that whereas both wild-type and mutant proteins are stable and monomeric over short time periods, the mutants can oligomerize into dimers and higher-order oligomers over longer times.

Discussion

Stability, unfolding, and dynamics of wild-type UCH-L1

Chemical denaturation experiments were used to establish that UCH-L1 can be reversibly unfolded *in vitro* and that it is a very stable protein with a free energy of unfolding of some 13–14 kcal mol^{-1} between the native state and the denatured state under the conditions used. The unfolding was found to be three-state, and an intermediate was populated at moderate concentrations of urea. Although a large degree of the structure has been lost upon unfolding to the intermediate state (approximately 60% of the native structure and probably most of the helical structure, as shown by far-UV CD), the intermediate remains compact and stable with respect to the denatured state.

The NMR HDX results are the most useful in terms of providing information on the structure of this intermediate state. Although our current HDX data cannot be converted into residue-specific free energies of unfolding due to the pH-dependent stability of UCH-L1, we have identified a significant number of residues that exhibit high protection factors in wild type (Fig. 5), and their high degree of protection suggests that the corresponding amide groups are protected from exchange in the intermediate state and therefore are likely to be in stable elements of secondary structure. These results indicate that the central part of the β-sheet, comprising residues in

Please cite this article as: Andersson, F. I. *et al.*, The Effect of Parkinson's-Disease-Associated Mutations on the Deubiquitinating Enzyme UCH-L1, *J. Mol. Biol.* (2011), doi:10.1016/j.jmb.2010.12.029

β-strands 2–4 and 6, is structured in the intermediate state, and that this β-sheet region is stabilized by some tertiary interactions with α-helices 3 and 7, and Leu3 in an N-terminal coil region, all of which still have one or two residues with high protection factors. The HDX data suggest that most of the residues in α-helices 3 and 7 do not retain structure in the intermediate state; thus, these results are compatible with the far-UV CD urea denaturation experiments, which show that most of the helical structure is lost in the transition from the native state to the intermediate state.

^{15}N spin relaxation measurements were employed to probe the internal motions of UCH-L1 variants on a fast nanoseconds timescale. The results show that the backbone motions are very similar across the primary sequence of UCH-L1, with the exception of the residues located in the C-terminal part of the cross-over loop (residues 150–160), which are significantly more flexible than the rest of the molecule (Fig. S6). From the NMR dynamics studies, we are also able to say that wild-type UCH-L1 is predominantly monomeric under the experimental conditions used. This is consistent with the SEC results, which show that unless the sample is kept at elevated temperatures for long periods, the wild-type protein is stable and monomeric (Fig. S7).

The effect of S18Y on the structure and stability of UCH-L1

Over the past decade, much work has been performed to establish whether there is a link between the S18Y polymorphism in UCH-L1 and susceptibility towards a number of neurodegenerative diseases, including PD, AD, and Huntington's disease. The main focus has been on PD, but different studies have produced conflicting results, and it is still unclear whether the S18Y mutation is a genetic modifier of these disease states (see Supporting Information for a full description of these studies).

A number of studies have attempted to address the effect of the S18Y mutation on the structure and function of UCH-L1 both *in vitro* and *in vivo*. In 2002, Liu *et al.* reported that UCH-L1 has a dimerization-dependent ubiquityl ligase activity, in addition to the hydrolase activity of the monomer.[27] While the S18Y mutation was found to have little effect on hydrolase activity, it was found to reduce ligase activity.[27] Nishikawa *et al.* also showed that S18Y has little effect on the hydrolase activity of UCH-L1, and they also determined that it did not have a significant effect on the structure, as shown by far-UV CD.[26] A follow-up study on the structure of S18Y using small-angle neutron scattering reported that both wild-type and mutant UCH-L1 were dimers at the concentrations used and that, compared to wild type and I93M, S18Y had a more globular structure within the dimer, similar to that observed in the crystalline state.[28] More recently, overexpression of S18Y, but not wild-type UCH-L1, was shown to confer an antioxidant function to neuronal cells.[29]

Here, we have undertaken a detailed biophysical characterization of S18Y in order to see if, and how, this mutation perturbs the structure and function of the protein. The stability measurements show that the mutation is slightly destabilizing, and that it specifically destabilizes the native structure. This appears to be the major impact of the mutation, as the structure (as shown by fluorescence, far-UV CD, and NMR) is hardly perturbed. In addition, the dynamics of S18Y are also very similar to those of the wild-type protein. These results are consistent with those reported by Naito *et al.* based on small-angle neutron scattering experiments.[28] However, in contrast to their results and to the report of Liu *et al.*, we find no evidence that the wild type or this mutant can form dimers unless left for long periods.[27]

Together with previous results, which have shown that S18Y has a hydrolase activity similar to that of wild type,[26,27] our results show that the protein is minimally perturbed compared to wild type, and that the primary effect of the mutation is to slightly reduce stability while having very little effect on structure. Given the similarities between S18Y and wild type, we find no evidence that would suggest that S18Y may behave in such a way as to contribute to a decreased susceptibility towards PD. However, without further extensive *in vitro* and *in vivo* studies, we do not rule out this possibility altogether.

The effect of I93M on the structure and stability of UCH-L1

The I93M mutation in UCH-L1 has been associated with an autosomal dominant form of PD.[13] Although early studies showed that the mutation resulted in a decrease in hydrolytic activity *in vitro*,[13,26] Yasuda *et al.*,[14] Setsuie and Wada,[30] Setsuie *et al.*,[31] Kabuta *et al.*,[32,33] and Kabuta and Wada[34] proposed that I93M acts by a gain of toxic function rather than by a loss of function.

Here, we have combined different biophysical techniques to study the effect of the I93M mutation on the structure and stability of UCH-L1. The urea unfolding experiments show that the mutant is less stable than the wild-type protein. The decrease in stability is also manifest in kinetic unfolding measurements, and I93M unfolds approximately 10-fold faster than wild type. In line with chemical denaturation experiments, I93M exhibits an overall decrease in HDX protection factors compared to those of wild type. Of interest is the fact that the exchange rates that have been most perturbed by mutation are from residues located in either α-helix

Please cite this article as: Andersson, F. I. *et al.*, The Effect of Parkinson's-Disease-Associated Mutations on the Deubiquitinating Enzyme UCH-L1, *J. Mol. Biol.* (2011), doi:10.1016/j.jmb.2010.12.029

3 or α-helix 1 (where the S18Y mutation lies), suggesting some longer-range effects of the mutation. In addition, while many of the exchange rates are faster in I93M than in wild type, indicating destabilization, there are a number of residues that have slower rates of exchange, reflecting a local stabilization of structure on mutation. In particular, the protection factors for Phe133 and Glu134 in I93M are significantly higher than their counterparts in wild type (Fig. 5). This can be attributed to structural rearrangements around the mutation site.

Our MD simulation suggests that the longer methionine side chain in the mutant may displace packing around the mutation site, leading to the loss of hydrophobic contacts with Met82 and new hydrophobic contacts with Gln84 and Phe133 (Fig. S5). The changes in side-chain packing explain the observed ^{1}H, ^{15}N, and ^{13}C chemical shift changes (Fig. 4; Fig. S4). During the course of our MD simulations, the crystal structure of I93M UCH-L1 was reported (Protein Data Bank entry 3IRT).[35] The crystal structures of wild type and I93M are very similar, with a root-mean-square displacement of 0.54 Å for all backbone C^{α} atoms. In particular, α-helices 5 and 6 of I93M are essentially identical with those in the wild-type structure. The Phe133 side chains in both variants exhibit identical configurations after superposition of the complete backbone structures. Similarly, the loop structures around Met82 and Lys83, including side chains, are very similar in both structures. However, both helices 5 and 6 are involved in packing in the crystal, and it is therefore possible that although the mutation may have somewhat perturbed these elements in solution, packing forces in the crystal have imposed a stabilizing influence, allowing these helices to retain the structure seen in the wild-type protein.

Given the biophysical data that we have presented here on I93M UCH-L1, it is possible to speculate on how this mutation may be linked to PD. We have shown that the mutation is destabilizing, and that it specifically destabilizes the native state. One consequence of this is that the intermediate state in I93M, which we have shown to be significantly unfolded, is more populated than that in wild type. This intermediate state may be the species that forms aberrant interactions with tubulin and with components of the chaperone-mediated autophagy machinery,[33] particularly as it is likely to expose the hydrophobic surface area that could interact with the chaperones Hsc70 and Hsp90. However, even I93M is a very stable protein with a free energy of unfolding of over 7 kcal mol^{-1} from the native state to the intermediate state, such that this intermediate state will only be very sparsely populated in the absence of denaturant. In addition, we have shown that the S18Y mutation is also destabilizing, although to a lesser extent than I93M, and it is clearly not associated with an increase in susceptibility to PD. Therefore, we conclude that loss of stability alone is not likely to be the cause of the neurodegeneration observed with I93M.

Although it has not been demonstrated directly here, previous work has established that while I93M shows decreased hydrolase activity relative to wild type,[26] this is not likely to be the cause of any disease state, as α-synuclein-induced dopaminergic cell loss is the same for wild-type UCH-L1 mice and transgenic mice, which do not express this enzyme.[14] Instead, we propose that the effects of I93M are due to the changes in structure that occur on mutation, as demonstrated here. Although these structural rearrangements may be small in scale, we propose that they result in the exposure of the hydrophobic surface area. This may have two consequences—firstly, the I93M mutant has an increased tendency towards aggregation *in vivo*, as has been observed in SH-SY5Y cells,[32] and, secondly, the exposure of the hydrophobic surface area may also lead to aberrant interactions with tubulin and with the chaperone-mediated autophagy machinery, as observed by other groups.[33] It is also interesting to speculate that the structural rearrangement may also make I93M UCH-L1 more readily modified by α,β-unsaturated carbonyls and other reactive species present in cells, particularly those undergoing oxidative stress. Such chemical modification of UCH-L1 has also been associated with a number of neurodegenerative diseases, including PD and AD.[16]

Materials and Methods

Materials

Glutathione fast-flow columns were purchased from GE Healthcare. Urea (ultra purity >99.5%) was purchased from Fluka, and all other chemicals were of analytical grade and purchased from Sigma-Aldrich.

Protein preparation

The pGEX-6-*uch-l1* constructs for wild-type, S18Y, and I93M UCH-L1 were made by Das *et al.* using standard molecular techniques.[18] Wild-type and mutant UCH-L1 were expressed and purified as previously described[18] (further details are available in Supporting Information).

Biophysical studies

All biophysical measurements were performed at 25 °C in 50 mM Tris (pH 7.6), 0.5 mM ethylenediaminetetraacetic acid, and 5 mM DTT, unless stated otherwise. Under these conditions, both wild type and mutants are monomeric, and the unfolding is independent of protein concentration (see Supporting Information for further details).

Please cite this article as: Andersson, F. I. *et al.*, The Effect of Parkinson's-Disease-Associated Mutations on the Deubiquitinating Enzyme UCH-L1, *J. Mol. Biol.* (2011), doi:10.1016/j.jmb.2010.12.029

Solution-state NMR spectroscopy

Backbone resonance assignments, HDX experiments, and ^{15}N backbone relaxation measurements were all performed using standard methods described in detail in Supporting Information.

MD simulations

The crystal structure of wild-type UCH-L1 (Protein Data Bank entry 2ETL[18]) was used as the starting structure for MD simulations with explicit solvent.[36] The point mutation of I93M was introduced *in silico* by modifying the coordinates for model generations and standard packages used for the simulations (further details are given in Supporting Information).

Measurement of protein stability: Equilibrium unfolding experiments

All equilibrium urea unfolding measurements were performed as described previously[20] using both fluorescence and far-UV CD, as described in Supporting Information.

Unfolding kinetics

The unfolding kinetics of wild-type and mutant UCH-L1 were measured by stopped-flow techniques for shorter timescales or by manual mixing with a fluorometer for longer timescales, as previously described[20] (further details are available in Supporting Information).

Acknowledgements

F.I.A. and S.E.J. acknowledge funding from the Leverhulme Trust. E.F.W.'s PhD studentship was funded by the Biotechnology and Biological Sciences Research Council. S.-T.D.H. is a recipient of the Human Frontier Science Program Long-Term Fellowship (LT0798/2005) and Career Development Award (CDA00025/2010) and is supported in part by the National Science Council of the Republic of China, Taiwan (NSC99-2911-I-007-034). We thank the staff of the Biomolecular NMR Facility and the University of Cambridge Department of Chemistry for their valuable assistance. Financial support was provided through access to research infrastructures activity in the 6th Framework Program of the European Community (contract no. RII3-026145, EU-NMR) for the conduct of the experiments at the Institute of Structural Biology (Grenoble, France). Moreover, the authors are very thankful to Dr. Adrien Favier and Dr. Bernhard Brutscher for excellent technical support.

Supplementary Data

Supplementary data to this article can be found online at doi:10.1016/j.jmb.2010.12.029

References

1. Komander, D., Clague, M. J. & Urbe, S. (2009). Breaking the chains: structure and function of the deubiquitinases. *Nat. Rev. Mol. Cell Biol.* **10**, 550–563.
2. Wilkinson, K. D. (2009). DUBs at a glance. *J. Cell Sci.* **122**, 2325–2329.
3. Reyes-Turcu, F. E., Ventii, K. H. & Wilkinson, K. D. (2009). Regulation and cellular roles of ubiquitin-specific deubiquitinating enzymes. *Annu. Rev. Biochem.* **78**, 363–397.
4. Komander, D. (2009). The emerging complexity of protein ubiquitination. *Biochem. Soc. Trans.* **37**, 937–953.
5. Nijman, S. M. B., Luna-Vargas, M. P. A., Velds, A., Brummelkamp, T. R., Dirac, A. M. G., Sixma, T. K. & Bernards, R. (2005). A genomic and functional inventory of deubiquitinating enzymes. *Cell*, **123**, 773–786.
6. Yamazaki, T., Hibi, K., Takase, T., Tezel, E., Nakayama, H., Kasai, Y. *et al.* (2002). PGP9.5 as a marker for invasive colorectal cancer. *Clin. Cancer Res.* **8**, 192–195.
7. Sasaki, H., Yukiue, H., Moriyama, S., Kobayashi, Y., Nakashima, Y., Kaji, M. *et al.* (2001). Expression of the protein gene product 9.5, PGP9.5, is correlated with T-status in non-small cell lung cancer. *Jpn. J. Clin. Oncol.* **31**, 532–535.
8. Hibi, K., Liu, Q., Beaudry, G. A., Madden, S. L., Westra, W. H., Wehage, S. L. *et al.* (1998). Serial analysis of gene expression in non-small cell lung cancer. *Cancer Res.* **58**, 5690–5694.
9. Wilkinson, K. D., Lee, K., Deshpande, S., Duerksen-hughes, P., Boss, J. M. & Pohl, J. (1989). The neuron-specific protein Pgp-9.5 is a ubiquitin carboxyl-terminal hydrolase. *Science*, **246**, 670–673.
10. Cartier, A. E., Djakovic, S. N., Salehi, A., Wilson, S. M., Masliah, E. & Patrick, G. N. (2009). Regulation of synaptic structure by ubiquitin C-terminal hydrolase L1. *J. Neurosci.* **29**, 7857–7868.
11. Saigoh, K., Wang, Y. L., Suh, T. G., Yamanishi, T., Sakai, Y., Kiyosawa, H. *et al.* (1999). Intragenic deletion in the gene encoding ubiquitin carboxy-terminal hydrolase in gad mice. *Nat. Genet.* **23**, 47–51.
12. Smith, D. L., Pozueta, J., Gong, B., Arancio, O. & Shelanski, M. (2009). Reversal of long-term dendritic spine alterations in Alzheimer disease models. *Proc. Natl Acad. Sci. USA*, **106**, 16877–16882.
13. Leroy, E., Boyer, R., Auburger, G., Leube, B., Ulm, G., Mezey, E. *et al.* (1998). The ubiquitin pathway in Parkinson's disease. *Nature*, **395**, 451–452.
14. Yasuda, T., Nihira, T., Ren, Y. R., Cao, X. Q., Wada, K., Setsuie, R. *et al.* (2009). Effects of UCH-L1 on alpha-synuclein over-expression mouse model of Parkinson's disease. *J. Neurochem.* **108**, 932–944.
15. Lowe, J., McDermott, H., Landon, M., Mayer, R. J. & Wilkinson, K. D. (1990). Ubiquitin carboxyl-terminal hydrolase (Pgp 9.5) is selectively present in ubiquitinated inclusion-bodies characteristic of human neurodegenerative diseases. *J. Pathol.* **161**, 153–160.

Please cite this article as: Andersson, F. I. *et al.*, The Effect of Parkinson's-Disease-Associated Mutations on the Deubiquitinating Enzyme UCH-L1, *J. Mol. Biol.* (2011), doi:10.1016/j.jmb.2010.12.029

16. Choi, J., Levey, A. I., Weintraub, S. T., Rees, H. D., Gearing, M., Chin, L. S. & Li, L. (2004). Oxidative modifications and down-regulation of ubiquitin carboxyl-terminal hydrolase L1 associated with idiopathic Parkinson's and Alzheimer's diseases. *J. Biol. Chem.* **279**, 13256–13264.
17. Koharudin, L. M., Liu, H., Di Maio, R., Kodali, R. B., Graham, S. H., Gronenborn, A. M. *et al.* (2010). Cyclopentenone prostaglandin-induced unfolding and aggregation of the Parkinson disease-associated UCH-L1. *Proc. Natl Acad. Sci.* **107**, 6835–6840.
18. Das, C., Hoang, Q. Q., Kreinbring, C. A., Luchansky, S. J., Meray, R. K., Ray, S. S. *et al.* (2006). Structural basis for conformational plasticity of the Parkinson's disease-associated ubiquitin hydrolase UCH-L1. *Proc. Natl Acad. Sci. USA*, **103**, 4675–4680.
19. Virnau, P., Mirny, L. A. & Kardar, M. (2006). Intricate knots in proteins: function and evolution. *PLoS Comput. Biol.* **2**, 1074–1079.
20. Andersson, F. I., Pina, D. G., Mallam, A. L., Blaser, G. & Jackson, S. E. (2009). Untangling the folding mechanism of the 5(2)-knotted protein UCH-L3. *FEBS J.* **276**, 2625–2635.
21. Andersson, F. I., Jackson, S. E. & Hsu, S. T. D. (2010). Backbone assignments of the 26 kDa neuron-specific ubiquitin carboxyl-terminal hydrolase L1 (UCH-L1). *Biomol. NMR Assign.* **4**, 41–43.
22. Tanford, C. (1968). Protein denaturation. *Adv. Protein Chem.* **23**, 121–282.
23. Orte, A., Craggs, T. D., White, S. S., Jackson, S. E. & Klenerman, D. (2008). Evidence of an intermediate and parallel pathways in protein unfolding from single-molecule fluorescence. *J. Am. Chem. Soc.* **130**, 7898–7907.
24. Mallam, A. L. & Jackson, S. E. (2006). Probing nature's knots: the folding pathway of a knotted homodimeric protein. *J. Mol. Biol.* **359**, 1420–1436.
25. Mallam, A. L. & Jackson, S. E. (2007). A comparison of the folding of two knotted proteins: YbeA and YibK. *J. Mol. Biol.* **366**, 650–665.
26. Nishikawa, K., Li, H., Kawamura, R., Osaka, H., Wang, Y. L., Hara, Y. *et al.* (2003). Alterations of structure and hydrolase activity of parkinsonism-associated human ubiquitin carboxyl-terminal hydrolase L1 variants. *Biochem. Biophys. Res. Commun.* **304**, 176–183.
27. Liu, Y. C., Fallon, L., Lashuel, H. A., Liu, Z. H. & Lansbury, P. T. (2002). The UCH-L1 gene encodes two opposing enzymatic activities that affect alpha-synuclein degradation and Parkinson's disease susceptibility. *Cell*, **111**, 209–218.
28. Naito, S., Mochizuki, H., Yasuda, T., Mizuno, Y., Furusaka, M., Ikeda, S. *et al.* (2006). Characterization of multimetric variants of ubiquitin carboxyl-terminal hydrolase L1 in water by small-angle neutron scattering. *Biochem. Biophys. Res. Commun.* **339**, 717–725.
29. Kyratzi, E., Pavlaki, M. & Stefanis, L. (2008). The S18Y polymorphic variant of UCH-L1 confers an antioxidant function to neuronal cells. *Hum. Mol. Genet.* **17**, 2160–2171.
30. Setsuie, R. & Wada, K. (2007). The functions of UCH-L1 and its relation to neurodegenerative diseases. *Neurochem. Int.* **51**, 105–111.
31. Setsuie, R., Wang, Y. L., Mochizuki, H., Osaka, H., Hayakawa, H., Ichihara, N. *et al.* (2007). Dopaminergic neuronal loss in transgenic mice expressing the Parkinson's disease-associated UCH-L1 193M mutant. *Neurochem. Int.* **50**, 119–129.
32. Kabuta, T., Setsuie, R., Mitsui, T., Kinugawa, A., Sakurai, M., Aoki, S. *et al.* (2008). Aberrant molecular properties shared by familial Parkinson's disease-associated mutant UCH-L1 and carbonyl-modified UCH-L1. *Hum. Mol. Genet.* **17**, 1482–1496.
33. Kabuta, T., Furuta, A., Aoki, S., Furuta, K. & Wada, K. (2008). Aberrant interaction between Parkinson disease-associated mutant UCH-L1 and the lysosomal receptor for chaperone-mediated autophagy. *J. Biol. Chem.* **283**, 23731–23738.
34. Kabuta, T. & Wada, K. (2008). Insights into links between familial and sporadic Parkinson's disease. *Autophagy*, **4**, 827–829.
35. Boudreaux, D. A., Maiti, T. K., Davies, C. W. & Das, C. (2010). Ubiquitin vinyl methyl ester binding orients the misaligned active site of the ubiquitin hydrolase UCHL1 into productive conformation. *Proc. Natl Acad. Sci.* **107**, 9117–9122.
36. Hsu, S. T. D. & Bonvin, A. M. J. J. (2004). Dynamics of CD4 binding-induced conformational changes in HIV gp120. *Proteins*, **55**, 582–593.

Please cite this article as: Andersson, F. I. *et al.*, The Effect of Parkinson's-Disease-Associated Mutations on the Deubiquitinating Enzyme UCH-L1, *J. Mol. Biol.* (2011), doi:10.1016/j.jmb.2010.12.029